(2)

A 154-DAY PERIODICITY IN THE OCCURRENCE RATE OF PROTON FLARES

T. Bai
Stanford University, Stanford, CA
and
E. W. Cliver
Geophysics Laboratory (AFSC)
Hanscom Air Force Base, Bedford, MA

To be published in the *Astrophysical Journal*

Supported by
NASA Grant NGL 05-020-272
NASA Contract NASA 8-37334
ONR Contract N00014-85-K-0111

A 154-DAY PERIODICITY IN THE OCCURRENCE RATE OF PROTON FLARES

T. Bai

Stanford University, Stanford, CA

and

E. W. Cliver

Geophysics Laboratory (AFSC)

Hanscom Air Force Base, Bedford, MA

ABSTRACT

We have analyzed periodicities in the occurrence rate of proton flares for solar cycles 19 through 21 (1955-86) and have identified two epochs that exhibit a 154-day periodicity. These epochs are a 14-year interval from 1958 January through 1971 December and a 5.5-year interval from 1978 February to 1983 August. The best-determined period is 154.6(±0.6) days. We have found that the phase of this periodicity changed between the above-mentioned two epochs by about one half of a period ($\Delta\phi$=0.5±0.16). It appears that the occurrence rate of proton flares is more sensitive to the 154-day periodicity than the occurrence rate of flares selected by other criteria.

I. INTRODUCTION

A periodicity of about 154 days was discovered by Rieger et al. (1984) in the occurrence rate of gamma-ray flares detected by the Gamma-Ray Spectrometer aboard the *Solar Maximum Mission* (*SMM*). They also found the same periodicity in the occurrence rate of flares with a soft X-ray classification above M4. This periodicity was confirmed by Kiplinger et al. (1984) who analyzed flares detected by the Hard X-Ray Burst Spectrometer aboard *SMM,* and has subsequently been found in the occurrence rates of flares selected by various observational criteria: microwave flux (Bogart and Bai 1985), Hα importance (Ichimoto et al. 1985), Hα flare index (Ozguc and Atac 1989), and production of interplanetary energetic electrons (Droge et al. 1989). This periodicity has been found not only in flare data but also in various indicators of solar activity such as the sunspot blocking function and the 10.7-cm flux from the whole Sun (Lean and Brueckner 1989).

After the discovery of the 154 day periodicity in the flare data of solar cycle 21, many people studied the periodicity in the activity data of cycle 20 (Bogart and Bai 1985; Ichimoto et al. 1985; Ozguc and Atac 1989). Although one finds a peak near 154 days in each power spectrum for cycle 20, in general, the peak near 154 days is weaker for cycle 20 than that for cycle 21. Lean and Brueckner (1989) analyzed various activity data for cycles 19 through 21. For cycle 21 they found a large peak near 158 days in the power spectra of the sunspot blocking function and the whole-Sun 10-cm radio flux. Similar results are obtained for cycle 20, but for cycle 19 a small peak near 159 days was found only in the spectrum of sunspot blocking function.

By analyzing the relationship between the 154-day periodicity and the distribution of flares on the Sun, Bai and Sturrock (1987) have shown the following. (a) This periodicity is not a local, but a global phenomenon.

Therefore, its mechanism must involve the whole Sun. (b) This periodicity is not due to the interaction of hot spots rotating at slightly different rates such that they overlap once every 154 days. (c) This periodicity is not caused by the interaction of "active bands," which are proposed (Wolff 1983) to be produced by g-mode oscillations of different l numbers.

Thus, the cause of the 154-day periodicity is still not understood. In order to gain insights on this problem, in the present paper we analyze the occurrence of energetic flares that produced interplanetary (IP) energetic protons, for cycles 19 through 21 (1955-86). In the same spirit, Kile, Cliver, and Fourgere (1990) analyze the occurrence rate of flares selected by 10-cm radio fluxes, for the same time interval. The preliminary results of these works have been reported by Bai, Cliver, and Kile (1990).

In Section II we discuss the event selection criteria. In Section III we discuss various methods of analyzing periodicity. In Section IV the results of our analyses are presented. In Section V we discuss and summarize the results.

II. PROTON EVENT SELECTION: SOURCES AND PROCEDURE

a) 1955-1969 Interval

For these years, we used the *Catalog of Solar Particle Events 1955-1969* (Svestka and Simon 1975) as a data source. The proton events in this catalog are classified according to the three-digit classification system of Smart and Shea (1971) which is partially reproduced in Table 1. The first digit corresponds to the logarithm of the peak ≥ 10 MeV flux (protons cm^{-2} s^{-1} sr^{-1}) measured by a near-Earth satellite. The second digit represents the 30 MHz absorption measured by a sunlit polar riometer, and the third digit

represents the response of a high latitude sea level neutron monitor. The classification system was constructed so that an event with a first digit of "1," for example, can be expected to also have second and third digits of "1." For our event list, we selected all events in the catalog with a first digit ≥ 0, or, when satellite measurements were not available as indicated by a first digit of "X," we selected events with second or third digits > 0. In general, then, the threshold flux for our event selection corresponds to a peak flux of > 10 MeV protons (J(> 10 MeV)) ≥ 1 proton cm^{-2} s^{-1} sr^{-1}, except for the period mainly before 1960, when less sensitive ground-based measurements were used and the effective threshold was J(>10 MeV) ≥ 10 proton cm^{-2} s^{-1} sr^{-1}.

Additional procedural details are as follows: (1) If the flare association for a proton event given in the catalog was characterized as "probable" or "certain," then the date of the flare was used for our list. If the flare association was only considered to be "possible," or if the responsible flare was thought to have occurred behind-the-limb and no flare time could be specified, then the date of the particle event onset was used. (2) If a proton event had both prompt and delayed (sudden-commencement (SC)) associated components, both of which exceeded the flux threshold, only the prompt component was considered. (3) Events attributed, at the "probable" or "certain" level, to recurrent geomagnetic storms were not included in our list; proton events with "possible" sources in recurrent storms were included. (4) An event on 1967 July 7 that exceeded the flux threshold (J>1 proton cm^{-2} s^{-1} sr^{-1}), but was observed only by a *Pioneer* satellite located > 90^{o} from the Earth-Sun line was omitted from our final list of events.

b) 1970-1979 Interval

For these years, we used the *Catalog of Solar Proton Events 1970-1979* (Akinyan et al. 1982) as a data source. As the name indicates, this catalog is a continuation of the Svestka and Simon (1975) catalog, and the Smart and Shea (1971) classification system was used here also. Thus, our selection criteria for these years were identical to those used for the period 1955-1969.

c) 1980-1986 Interval

For these years, we used the *Eighth Interplanetary Monitoring Platform* (*IMP-8*) data on 20-40 MeV protons published in *Solar-Geophysical Data* (SGD). Assuming a "typical" E^{-3} energy spectrum (Van Hollebeke, Ma Sung, and McDonald, 1975), a proton event with a peak differential flux $\geq 10^{-2}$ protons cm^{-2} s^{-1} sr^{-1} MeV^{-1} will have an integral flux J(> 10 MeV) ≥ 1 proton cm^{-2} s^{-1} sr^{-1}. Thus, all events with J(20-40 MeV) ≥ 10^{-2} above background were included in the list. To eliminate "modulation events" (see Section IId), we required a factor of five increase to identify a new event when an event was in progress, i.e., when J(20-40 MeV) ≥ 10^{-2}. Also, consistent with the procedure for 1955-1979, additional SC-related peaks were excluded. The SGD plots were supplemented by higher time resolution plots courtesy of R. E. McGuire for the years 1980-1983.

d) Difficulties and Inconsistencies

The difficulties of compiling the list of proton events presented in the Svestka and Simon (1975) and Akinyan et al. (1982) catalogs are referred to in Akinyan et al. (p. 34).

> There are many particle increases which show two or more components in their development. *We consider them as two*

or more new events only if the sources of the components was identified successfully [italics added]. Otherwise the particle flux increase was listed as one event.

This technique eliminates spurious events that may represent only a modulation of previously accelerated particles. Some real events may also be omitted, however. To supplement both of the above catalogs, we used a recent compilation by Shea and Smart (1989) of proton events from 1955-1986 with J(> 10 MeV) ≥ 10 protons cm^{-2} s^{-1} sr^{-1} to make certain that no big events were left off our list. Eight events of a total of 385 were added in this manner.

For the years 1980-1986, we required J(> 10 MeV) ≥ 1 proton cm^{-2} s^{-1} sr^{-1} above background. This background subtraction was not done for the Svestka and Simon (1975) catalog. Akinyan et al. (1983) subtracted the background flux for isolated events and also for the initial component of compound events. Another source of inhomogeneity, mentioned above, in our final list of events involves the event selection threshold which is effectively higher for much of cycle 19 (before 1960) than for cycles 20 and 21. This higher effective threshold for the first half of cycle 19 is reflected in the number of events on our list from each solar cycle. For cycle 19 (nominally 1955-1964) we have 115 events, compared to 141 events for cycle 20 (1965-1975), and 129 events for cycle 21 through May 1986. The larger number of events in cycle 20 than in cycle 21 is mildly surprising, given the higher level of spottedness during cycle 21 (McKinnon 1987). The discrepancy may be due, at least in part, to our use of a single satellite for the years 1980-1986 (both the Svestka and Simon [1975] and Akinyan et al. [1983] catalogs considered multiple data sources) and the frequent gaps in *IMP* coverage during this period.

The dates of the proton flares we selected are listed in Table 2. As we have discussed above, proton-flare catalogs which we have used as data sources are based on observations by different detectors, and thus the event selection criteria we adopted are not exactly the same for the whole period. However, such changes are of much longer time scales than 154 days. Therefore, this does not influence the 154-day periodicity significantly.

III. METHODS OF PERIODICITY ANALYSIS

The standard method of periodicity analysis is the Fourier spectral analysis. The fast Fourier transformation (Cooley and Tukey 1965) is efficient and often used. The periodogram analysis (Scargle 1982) and the epoch folding method are also used. In the epoch folding method the period for which the phase diagram is the least uniform is searched for. In addition to these, the directionality analysis and the maximum likelihood method are used for periodicity analysis. In this section these latter two methods are discussed in more detail, because they are used in this paper and are perhaps less familiar to readers.

a) Directionality (Rayleigh Power Spectrum) Analysis

Suppose we want to determine whether n events with angular values of $\{\theta_1, \theta_2, \theta_3, ..., \theta_n\}$ are uniformly distributed in angle. We can represent each event as a unit vector $\mathbf{u}_i = cos\ \theta_i\, \mathbf{e}_x + sin\ \theta_i\, \mathbf{e}_y$, where $\mathbf{e}_x$ and $\mathbf{e}_y$ are unit vectors parallel to the X-axis and Y-axis, respectively. The vector sum of these unit vectors is given by

$$\mathbf{U} = \sum_{i=1}^{n} cos\ \theta_i\, \mathbf{e}_x + \sum_{i=1}^{n} sin\ \theta_i\, \mathbf{e}_y \qquad (1)$$

The magnitude of this vector divided by the number of events,

$$R = \frac{1}{n}\left\{\left(\sum_{i=1}^{n} \cos\theta_i\right)^2 + \left(\sum_{i=1}^{n} \sin\theta_i\right)^2\right\}^{1/2}, \tag{2}$$

indicates the uniformity of the distribution (Mardia 1972). If the events are uniformly distributed, R is very close to zero. If, on the other hand, the events are concentrated around a certain angle, R is close to 1. The direction angle of the vector **U** shows the angle around which the events are concentrated. If we define the quantity, z, as

$$z = nR^2 = \frac{1}{n}\left\{\left(\sum_{i=1}^{n} \cos\theta_i\right)^2 + \left(\sum_{i=1}^{n} \sin\theta_i\right)^2\right\}, \tag{3}$$

for randomly distributed events, the distribution of z follows $P(z>K)=exp(-K)$ (Mardia 1972). We obtain the "Rayleigh power spectrum" $z(\nu)$ by setting $\theta_i = 2\pi t_i/T = 2\pi\nu_i$, where $\{t_i\}$ is a set of flare occurrence times and T is a variable period (Droge et al. 1989).

b) Maximum Likelihood Method

Suppose the relative probability for flare occurrence is described by a sinusoidal distribution function,

$$P(t) = 1 + A \sin(2\pi t/T + \phi_0). \tag{4}$$

Here the mean probability is taken to be unity. Then, the joint probability of finding n flares with a set of occurrence times $\{t_1, t_2, t_3, \ldots, t_n\}$ is given by

$$M(T, A, \phi_0) = \prod_{i=1}^{n} \{1 + A \sin(2\pi t_i/T + \phi_0)\}. \tag{5}$$

This is a likelihood function. In the maximum likelihood method, we find the periodicity by finding the values of T, A, and ϕ_0 that maximize the

likelihood (e.g., Brandt 1976). If we take the logarithm of the above equation, we obtain a logarithmic likelihood function,

$$m(T, A, \phi_0)=\sum_{i=1}^{n} ln\{1+A\ sin\ (2\pi t_i / T+\phi_0)\}. \tag{6}$$

By determining the values of A and ϕ_0 that maximize the likelihood for various values of T, we can find the "likelihood power spectrum" $m_m(T)$ as a function the period T only.

c) Scargle's Periodogram

The periodogram is defined to be (Scargle 1982)

$$P_x(\omega)=\frac{1}{2}\left\{ \frac{\left[\sum_{i=1}^{N} X(t_i)\ cos\ \omega(t_i-\tau)\right]^2}{\sum_{i=1}^{N} cos^2\ \omega(t_i-\tau)} + \frac{\left[\sum_{i=1}^{N} X(t_i)\ sin\ \omega(t_i-\tau)\right]^2}{\sum_{i=1}^{N} sin^2\ \omega(t_i-\tau)} \right\}, \tag{7}$$

where $X(t_i)$ is a time series (series of measurements arranged in order of time) for $i=1, ..., N$, and τ is defined by the equation

$$tan\ 2\omega\tau = \sum_{i=1}^{N} sin\ 2\omega t_i \Big/ \sum_{i=1}^{N} cos\ 2\omega t_i .$$

d) Comparison of the above Methods

Scargle's method has several advantages over the conventional fast Fourier transformation method (Horne and Baliunas 1986). First, it is convenient for analysis of unevenly sampled data. Second, for purely independently and normally (Gaussian) distributed noise with zero mean and constant variance σ, the power distribution follows an exponential distribution (Knight, Schatten, and Sturrock 1979; Scargle 1982; Horne and

Baliunas 1986); i.e., the probability of the power density at a given frequency being greater than K by chance is given by

$$P(z>K) = exp\ (-K/\sigma^2) \qquad (8)$$

The directionality analysis method and the maximum likelihood method can be used only when the measurements are counts of discrete events. When this is the case, we can show that Scargle's periodogram is equivalent to the Rayleigh power spectrum. For a large number of evenly sampled time series,

$$\sum_{i=1}^{N} cos^2\ \omega\,(t_i-\tau) = \sum_{i=1}^{N} sin^2\ \omega\,(t_i-\tau) = \frac{N}{2}.$$

If we substitute this expression into equation (7), it becomes identical to equation (3) except for the phase angle and the multiplication factor. However, equation (3) is independent of the choice of the X axis (phase angle). The Rayleigh power spectrum is simpler to calculate, when the total event number n is smaller than the number of time series N.

The maximum likelihood method is cumbersome, because we have to explore the phase space made of several parameters. However, this method has a couple of advantages over other methods. First, in this method, we have flexibility in the choice of the distribution function. Instead of a sinusoidal distribution function given by equation (4), we can use a step function, for example, if there is a good reason for it. Second, the logarithmic likelihood function is cumulative. We will make use of this in the next section.

By applying the above three methods and the Fourier spectral analysis to the same set of data, we have confirmed that they all give almost identical results, except for normalization. If we use the sinusoidal

probability given by equation (4), the likelihood function as a function of period (or frequency) turns out to be similar to the Rayleigh power spectrum not only in shape but also in magnitude. As we discussed earlier, the Rayleigh power spectrum is supposed to be normalized, when the occurrences of all events are independent. We have confirmed this by Monte Carlo simulations. However, the occurrences of proton flares are not independent, because some active regions produce more than one proton flare. Owing to this, as we shall see in the next section, the Rayleigh power spectrum is not normalized. Droge et al. (1989) did not take this effect into account in estimating the statistical significance of the 154-day periodicity of "electron flares."

Even if we use a normalized time series,

$$X_i'=(X_i-X_{av})/\sigma,$$

where X_i is the number of proton flares on the i*th* day, X_{av} is the average daily proton flare number, and σ is the variance, because of the interdependence of occurrences of some proton flares, the Scargle's periodogram turns out to be not normalized. Therefore, whatever analysis method is used, the best way to normalize the power spectrum is to fit the actual power distribution to equation (8).

IV. ANALYSIS

a) Solar Cycle 21

Because the 154-day periodicity was initially found in the activity data of solar cycle 21, we first discuss the results for cycle 21. Figure 1 shows the normalized power spectrum of the occurrence rate of proton flares for cycle

21 (a) and that for the time interval from 1978 February 15 to 1983 August 6 (b). The 154-day periodicity is found to be operative mainly in the latter interval during cycle 21, as shown below. For this figure power spectra were calculated for the 31-230 nHz (50-373 days) range with 1 nHz intervals.

Figure 2 shows the distribution of the Rayleigh power values corresponding to the normalized spectrum shown in Figure 1b. The vertical axis shows the cumulative number of frequencies for which the Rayleigh power exceeds a certain value. Of course, for all 200 frequencies the Rayleigh power exceeds 0; thus, we have a point at (X=0, Y=200). At only one frequency (75 nHz, which is equivalent to 154.3 days) the Rayleigh power was 14.2, its maximum value. For lower values of Rayleigh power, the distribution can be well fit by the equation Y = 200 exp(-X/1.70), as expected from equation (8). Thus, we normalize the power spectrum by dividing the Rayleigh powers by 1.70 to obtain Figure 1b. For other cases, we use the same procedure for normalization.

In estimating the statistical significance of the peaks in the power spectrum, the "false alarm probability" may be used. It is given by the expression,

$$F = 1 - [1 - exp(-z_m)]^N, \qquad (9)$$

where z_m is the height of the peak in the normalized power spectrum and N is the number of independent frequencies (Scargle 1982; Horne and Baliunas 1986). The interpretation of F is as follows. If we have a discrete power spectrum giving the power at each of N independent frequencies for a set of random data, F indicates the probability that the power at one or more of these frequencies will exceed z_m by chance. The number of independent frequencies is determined by $N=(f_1-f_2)/\Delta f_{ifs}$. Here f_1-f_2, is the

frequency range, and the independent Fourier spacing is given by $\Delta f_{ifs}=1/\tau$, where τ is the time span of the data.

For τ=5.5 years = 2008 days, $\Delta f_{ifs}=5.8\ nHz$. Thus, there are 34 independent frequencies in the 31-230 nHz interval. We over sampled to obtain the power spectrum shown in Figure 1b, in which the height of the peak at 154.3 days is 8.36. The over sampling tends to increase the peak value. Therefore, if we substitute z_m=8.36 and N=34 into equation (9), we underestimate the false alarm probability. However, if we substitute N=200 (since we searched 200 frequencies with 1 nHz intervals) into equation (9), it turns out that it adequately compensates the effect of increase of the peak value by over sampling. By using z_m=8.36 and N=200, we get F=0.046. Because we searched for the time interval which maximizes the value of the 154-day peak, we must include the effect of this search in estimating the false alarm probability. Even if the data set is random, we can increase the peak power somewhat by interval searching. By Monte Carlo simulations, we find that the effect is a reduction in the flase alarm probability by about 3. Therefore, we can conclude that the probability of obtaining by chance such a high peak as in Figure 1b in the 50-370 day interval is about 14%.

For the sake of comparison, we list in Table 3 the peak values of the normalized power for different data sets for cycle 21. For the case of HXRBS flares, we used flares with peak count rates > 1000 counts s^{-1} only. We used a uniform procedure to obtain the results. The peak value for proton flares is comparable to those for HXRBS flares and GRS flares but considerably smaller than that for electron flares. Since the proton flare occurrence rate conforms to the 154-day periodicity found from other data sets, it is reasonable to use the proton data to study the flare activity periodicity for earlier times.

In order to determine the time interval in which the 154-day periodicity was operative, we have used the fact that the logarithmic likelihood function is cumulative. We define $m(k)$ as follows:

$$m(k) = \sum_{i=257}^{k} ln\{1 + 0.45\, sin\,[2\pi(t_i - 8524)/154d + 0.5\pi]\}. \qquad (10)$$

Here we use T=154 d somewhat arbitrarily, and the phase and amplitude of the sinusoidal function are chosen to maximize the likelihood for k=385. (The 257th event since 1955 is the first event of cycle 21, and the 385th is the last.) If events occur at random phases, the value of $y=1+A\ sin\ (2\pi t/T+\phi_0)$ is 1 on the average, and thus the value of $ln\ y=ln\ \{1+A\ sin\ (2\pi t/T+\phi_0)\}$ is zero on the average. However, if event occurrences conform to the periodicity, more events occur when the value of $y=1+A\ sin\ (2\pi t/T+\phi_0)$ is bigger than 1. Thus, for time intervals when the proton flare occurrence rate conforms to the periodicity, $m(k)$ increases on the average as k increases; for time intervals when it does not conform to the periodicity, $m(k)$ fluctuates or decreases as k increases. Therefore, equation (10) provides a good way of determining when the periodicity is operative. In Figure 3 we find that $m(k)$ increases on the average for the interval between event numbers 270 and 370.

Figure 4 shows the flare occurrence rate as a function of time for the time interval from 1977 September 14 through 1984 November 9 (which includes events with event numbers 270-370). For this figure the occurrence rate has been smoothed with a triangular window function having a total duration of 61 days. The 154-day periodic modulation of the flare occurrence rate is semi-regular in the time interval from about 1978 February 15 to 1983 August 6. By analyzing the occurrence rate of the proton flares for this

epoch only, we find that the best determined period is 153.7±1.5 days (one sigma error). Hence, the vertical grid lines have been placed 153.7 days apart, and they are positioned such that the maximum phases of the periodicity fall in the middle of grid lines. This epoch corresponds to 13 cycles. The time of first maximum of the 154-day periodicity in this epoch is 1978 May 3 (t=8524 days since 1955 January 1), which is indicated by an arrow in Figure 4. *SMM* observations have shown that the 154-day periodicity repeated 8 cycles during the 1980-83 interval (Rieger et al. 1984; Dennis 1985). The present result extends the epoch for 154-day periodicity further back in time in cycle 21.

The 218-day peak in Figure 1a is comparable to the 154-day peak. However, interval searching described above does not increase the 218-day power appreciably. Inspection of the proton occurrence time profiles shows that the power for the 218 day peak is mainly contributed by four episodes (around t=8525, 9598, 10058, and 11357 days) of strong flare activity, which are separated by approximately integer multiples of 218 days. Therefore, we do not regard the 218-day periodicity statistically significant.

b) Solar Cycles 19 and 20

The power spectrum for cycles 19 and 20 combined is shown in Figure 5a. Using the analysis described above, the 154 day periodicity is found to be operative mainly in the interval from the beginning of 1958 to the end of 1971, and the power spectrum for this interval is shown in Figure 5b. The normalized height of the 154-day peak is 7.62 for Figure 5a and 11.68 for Figure 5b. The false alarm probability of obtaining by chance a peak with z_m=11.68 in the 31-230 nHz (50-370 days) interval by chance is only 0.2%. The probability of obtaining such a high peak in the neighborhood of 154 days by

chance is considerably smaller (of order of 10^{-5}). If we perform the spectral analysis for cycle 19 and cycle 20 separately, the normalized heights of the 154-day peaks are 3.0 and 5.5, respectively. Because the epoch for the 154-day periodicity is stretched over a part of cycle 19 and a part of cycle 20, he 154-day peaks for individual cycles become statistically insignificant.

Figure 6 shows the proton flare occurrence rate as a function of time for the interval from 1958 January 1 through 1972 May 22. The occurrence rate has been smoothed with a triangular window function having a total duration of 61 days. The proton flare occurrence rate shows a semi-regular 154-day periodic for the 14-year time interval from 1958 through 1971 (except for few cycles). This interval corresponds to 33 cycles. (In comparison, the 11-year solar cycle, admittedly a more regular phenomenon, is in its 27th repetition after the Maunder minimum.) The best-determined period for this epoch is 154.6±0.6 days (one sigma error); hence the vertical grid lines are 154.6 days apart. From the phase angle calculation, we find that the time of the first maximum of the 154-day periodicity in this epoch is 1958 March 25 (t=1180 days since 1955 January 1), which is indicated by an arrow in Figure 6.

c) Phase shift

We have found that the 154-day periodicity is operative mainly in two epochs: from 1958 January to 1971 December and from 1978 February to 1983 August. Figure 7 shows the annual number of proton flares for the 32 years from 1955 through 1986. The two epochs for the 154-day periodicity are shown with horizontal lines. Because the first epoch covers the maxima of two solar cycles, we can infer that the 154-day periodicity is not a phenomenon subordinate to the 11-year cycle.

The best-determined period is 154.6±0.6 days for the first epoch and 153.7±1.5 days for the second epoch, and they are in agreement within the errors. Now let us study the phase relationship between the 154-day periodicity in these two epochs. The time of the first maximum of the periodicity in the first epoch is 1180 days, and that for the second epoch is 8524 days. We find that the time interval between them is 47.5 times 154.6 days; i.e., 8524-1180=154.6x47.5. Thus, we find that a phase shift of about 0.5 (180°) has occurred to the periodicity between the two epochs. Considering the uncertainty of the period 154.6±0.6 days, the phase shift is between 0.32 and 0.69.

We can calculate the phase shift, by calculating the Rayleigh power after adding a variable time shift Δt to the occurrence times of the proton flares of cycle 21. Then, the Rayleigh power near 154 days is a function of both period and time shift. We have found that the Rayleigh power attains the maximum value when the period T=154.6 days and Δt=77 days. Thus, the 154.6-day periodicity of cycle 21 is phase-shifted by about 0.5 ($\Delta\phi$=77/154.6=0.5) with respect to that of the earlier epoch. The black dot in Figure 8 indicates the location where the Rayleigh power attains the maximum, and the contour line shows a 1-σ range. (In estimating the 1-σ range, we have taken into account the proper normalization of the power spectrum.) Thus, T=154.6(±0.6) days, and $\Delta\phi$=0.5±0.16. This result agrees with the above result from the straightforward method. Our analysis shows that the hypothesis of a phase shift of 0.5 is 73 times more likely than the hypothesis of no phase shift.

Figure 9 shows the phase diagrams for the above-mentioned two epochs when the 154.6-day periodicity was operative. We find that the amplitudes of the modulation of the flare rate are large; it changes by a

factor of 6 from peak to valley. We also find a phase shift of about 0.5 between the two phase diagrams, in agreement with Figure 8. Bogart and Bai (1985) claimed that the phase of the 154-day periodicity remained coherent from cycle 20 to cycle 21. However, because the uncertainty of the period is large for their result (about 2 days), the phase coherency cannot be determined. The uncertainty of the period is only 0.6 days for the present result because of the long duration of the first epoch for the 154-day periodicity, and thus we can study the phase shift meaningfully.

For comparison with Figures 4 and 6, in Figure 10 we plot the proton flare occurrence rate for the interval from the beginning of 1972 through the end of 1977. According to the above discussions, the proton flare occurrence in this interval does not conform to the 154.6-day periodicity. The power spectrum for this interval is found not to have any statistically significant peaks.

V. DISCUSSION

a) Comparison with Other Results

The 154-day periodicity found in the proton flare occurrence rate of cycle 21 is consistent with the results from other data sets. Initially this periodicity was found to repeat 8 cycles during 1980-83. Whether this periodicity commenced before 1980 cannot be answered by analyzing SMM observations, which began in 1980 February. From the time profile of microwave flares (Fig. 1 of Bogart and Bai 1985), we find that this periodicity began to operate in 1980 for microwave flares. The present study, however, shows that the 154-day periodicity was operative since 1978 February for 13 or 14 cycles.

The 154-day periodicity of the proton flare occurrence was semi-regular in the interval from the beginning of 1958 to the end of 1971 during cycles 19 and 20. The 154-day peak is statistically significant for this interval. However, 154-day peak becomes statistically insignificant, if we calculate the power spectra of proton flares for cycles 19 and 20 separately. This is because the epoch for the 154-day periodicity is stretched over the two solar cycles. This may be one of the reasons why the 154-day periodicity is not very significant in the power spectra of other data sets analyzed for cycle 20 alone.

While the 154-day periodicity is significant in the proton flare occurrence rate for the 1958-71 interval, the occurrence rate of flares selected by the 10-cm radio fluxes does not show any significant periodicity near 154 days in the same interval nor in cycle 20 (Kile, Cliver, and Fougere 1990). It is probable that the 154-day periodicity influences the occurrence rates of different types of flares differently.

Bai (1987) discovered a 51-day periodicity in the occurrence rate of major flares for cycle 19. The major flares in this study are flares with comprehensive flare indices (CFIs) greater than 5, which were selected from the compilations of Dodson and Hedeman (1971, 1975). Similarly, Kile, Cliver, and Fougere (1990) found a 51-day peak (at a less significant level) in the power spectrum of the occurrence rate of microwave (2.8 GHz) flares for this cycle. However, we do not find any statistically significant periodicity near 51 days in the proton flare rate of cycle 19 nor of any other cycles. Lean and Brueckner (1989) also did not find the 51-day periodicity in the power spectra for solar cycle 19. It is not clear why the proton flare rate, at least from 1958, and the sunspot blocking function exhibit the 154-day periodicity

during cycle 19, while the occurrence rate of flares selected by CFIs and microwave fluxes exhibit the 51-day periodicity during cycle 19.

Table 4 summarizes results of periodicity analyses by various authors using different observations. We see that the evidence of the 154-day periodicity has been found in several data sets for at least parts of cycles 19, 20, and 21. We also see that the 51 day periodicity has been found in two data sets for cycle 19. The 154-day periodicity could be regarded as a subharmonic of the 51-day periodicity. The 51-day periodicity has also been detected in the solar diameter measurements (Delache, Laclare, and Sadsaoud 1985).

From the above discussions, it appears that the occurrence rate of proton flares is more sensitive to the 154-day periodicity than flares selected by other criteria. This conclusion is based on the results of cycles 19 and 20 discussed above, in particular, the absence of evidence for the 154-day periodicity in the 10-cm burst and CFI data for the 1958-1971 epoch (Kile, Cliver, and Fourgere 1990). During cycle 21, the 154 day periodicity became operative since 1978 February in the proton flare occurrence rate, while it became apparent only after 1980 in the occurrence rate of flares selected by microwave emission.

b) Intermittence and Phase Shift

Perhaps the most important result of this work is that the 154-day periodicity is intermittent by showing up in two different epochs, and that the phase has changed by about 0.5 from one epoch to the next. Simple analogies may help illucidate the physical meaning of this finding. A damped linear oscillator can exhibit intermittence and a phase shift. When a damped linear oscillator is excited, it shows a periodic modulation with a

certain amplitude. As time goes on, its amplitude decays, and when the amplitude is comparable to the noise, the periodic modulation is no longer discernible. After another excitation of the oscillator, it again shows a periodic modulation. However, the later excitation is not necessarily in phase with the earlier periodic modulation.

The analogy to a damped linear oscillator, however, is not consistent with observations in the following aspects. First, we do not see any obvious sign of the monotonic decay of the amplitude in the flare rate shown in Figures 4 and 6. Also we see linear increases of the logarithmic likelihood with increasing event number in Figure 3. Second, the proton flare rate began to show the 154-day periodicity from 1978 February during cycle 21, but the rate of microwave flares began to show the periodicity only after 1980 January. Therefore, if anything, the periodicity was stronger (or more influential) during the 1980-83 interval than 1978-79 interval.

We can think of another analogy. A damped nonlinear oscillator with a periodic forcing term can show periodic behavior sometimes and chaotic behavior at other times. For example, the damped, periodically forced nonlinear oscillator described by so-called Duffing's equation,

$$\frac{d^2x}{dt^2}+k\frac{dx}{dt}+x^3=B\cos t, \qquad (11)$$

shows periodic behavior for certain values of parameters k and B, and chaotic behavior for slightly different values (Thompson and Stewart 1986). This oscillator can show an order 3 subharmonic periodicity as well as the fundamental periodicity. It is interesting to note that the 154-day periodicity can be interpreted as the order 3 subharmonic of the 51-day periodicity.

We wish to thank J. A. Klimchuk and J. N. Kile for helpful discussions and critical reading of the manuscript. Comments by an anonymous referee were helpful. The work at Stanford was supported by Office of Naval Research Contract N00014-85-K-0111, by NASA grant NGL 05-020-272, and as part of the Solar-A collaboration under NASA contract NASA 8-37334 with Lockheed Palo Alto Research Laboratories.

Table 1

Solar Proton Event Classification System (Smart and Shea 1971)

Digit	First	Second	Third
	>10 MeV proton flux (protons cm^{-2} s^{-1} sr^{-1})	Daylight polar cap absorption at 30 MHz (dB)	Sea level neutron monitor increase (%)
0	10^0 - $<10^1$	No measurable increase	No measurable increase
1	10^1 - $<10^2$	<1.5	<3
2	10^0 - $<10^1$	1.5 - <4.6	3 - <10
X	Measurement not available		

TABLE 2

DATES OF PROTON FLARES

No.	Dates	No.	Dates	No.	Dates	No.	Dates
1	55 Jan 16	48	58 Aug 22	95	61 Jul 12	142	67 Nov 2
2	56 Feb 23	49	58 Aug 26	96	61 Jul 15	143	67 Nov 11
3	56 Mar 10	50	58 Sep 22	97	61 Jul 18	144	67 Nov 13
4	56 Apr 27	51	59 Jan 26	98	61 Jul 20	145	67 Nov 15
5	56 Aug 31	52	59 Feb 12	99	61 Jul 24	146	67 Dec 3
6	56 Nov 13	53	59 May 10	100	61 Sep 7	147	67 Dec 16
7	57 Jan 20	54	59 Jun 9	101	61 Sep 10	148	67 Dec 17
8	57 Feb 21	55	59 Jun 12	102	61 Sep 28	149	67 Dec 17
9	57 Apr 3	56	59 Jul 10	103	61 Nov 10	150	67 Dec 18
10	57 Apr 6	57	59 Jul 14	104	62 Feb 1	151	67 Dec 30
11	57 Apr 11	58	59 Jul 16	105	62 Feb 4	152	68 Jan 12
12	57 Apr 17	59	59 Aug 18	106	62 Feb 20	153	68 Jan 12
13	57 May 8	60	59 Aug 18	107	62 Oct 23	154	68 Feb 8
14	57 May 19	61	59 Sep 1	108	63 Apr 15	155	68 Feb 17
15	57 Jun 19	62	60 Jan 11	109	63 Aug 6	156	68 Apr 26
16	57 Jun 22	63	60 Mar 30	110	63 Aug 9	157	68 Jun 9
17	57 Jun 30	64	60 Mar 30	111	63 Sep 15	158	68 Jul 6
18	57 Jul 3	65	60 Apr 1	112	63 Sep 16	159	68 Jul 8
19	57 Jul 24	66	60 Apr 5	113	63 Sep 20	160	68 Jul 12
20	57 Jul 28	67	60 Apr 28	114	63 Sep 26	161	68 Jul 12
21	57 Aug 9	68	60 Apr 29	115	64 Apr 16	162	68 Sep 26
22	57 Aug 27	69	60 May 4	116	65 Feb 5	163	68 Sep 28
23	57 Aug 28	70	60 May 6	117	65 Oct 4	164	68 Sep 29
24	57 Aug 29	71	60 May 9	118	66 Mar 24	165	68 Oct 3
25	57 Aug 31	72	60 May 13	119	66 May 2	166	68 Oct 23
26	57 Sep 2	73	60 May 17	120	66 Jul 7	167	68 Oct 29
27	57 Sep 11	74	60 May 26	121	66 Jul 9	168	68 Oct 30
28	57 Sep 18	75	60 Jun 1	122	66 Aug 28	169	68 Oct 30
29	57 Sep 21	76	60 Jun 25	123	66 Sep 2	170	68 Nov 1
30	57 Sep 26	77	60 Jun 27	124	66 Sep 4	171	68 Nov 4
31	57 Oct 20	78	60 Aug 11	125	66 Sep 4	172	68 Nov 18
32	57 Nov 4	79	60 Aug 14	126	66 Sep 14	173	68 Nov 20
33	57 Dec 16	80	60 Aug 26	127	66 Sep 14	174	68 Nov 21
34	57 Dec 28	81	60 Sep 3	128	67 Jan 28	175	68 Dec 2
35	58 Feb 9	82	60 Sep 26	129	67 Jan 28	176	69 Jan 17
36	58 Mar 11	83	60 Oct 3	130	67 Feb 2	177	69 Jan 24
37	58 Mar 14	84	60 Oct 29	131	67 Feb 27	178	69 Feb 25
38	58 Mar 17	85	60 Nov 10	132	67 Mar 11	179	69 Feb 26
39	58 Mar 23	86	60 Nov 11	133	67 May 23	180	69 Feb 27
40	58 Mar 30	87	60 Nov 12	134	67 May 28	181	69 Feb 28
41	58 Apr 10	88	60 Nov 14	135	67 Jun 3	182	69 Mar 12
42	58 Jun 4	89	60 Nov 15	136	67 Jun 6	183	69 Mar 17
43	58 Jun 6	90	60 Nov 19	137	67 Jun 12	184	69 Mar 21
44	58 Jul 7	91	60 Nov 20	138	67 Aug 1	185	69 Mar 30
45	58 Jul 29	92	60 Dec 5	139	67 Aug 3	186	69 Apr 10
46	58 Aug 16	93	61 Apr 13	140	67 Aug 4	187	69 Apr 24
47	58 Aug 19	94	61 Jul 11	141	67 Aug 9	188	69 May 13

No.	Dates	No.	Dates	No.	Dates	No.	Dates
189	69 Jun 7	239	72 Oct 29	288	78 Oct 8	337	81 Dec 27
190	69 Sep 25	240	72 Nov 2	289	78 Oct 9	338	82 Jan 2
191	69 Oct 14	241	73 Apr 11	290	78 Oct 17	339	82 Jan 30
192	69 Oct 14	242	73 Apr 29	291	78 Nov 10	340	82 Feb 1
193	69 Nov 2	243	73 Jul 29	292	78 Dec 11	341	82 Feb 8
194	69 Nov 7	244	73 Sep 7	293	79 Feb 16	342	82 Mar 7
195	69 Nov 24	245	74 Jul 2	294	79 Mar 1	343	82 Mar 30
196	69 Dec 18	246	74 Jul 4	295	79 Mar 9	344	82 Jun 3
197	69 Dec 20	247	74 Jul 5	296	79 Apr 3	345	82 Jun 27
198	69 Dec 30	248	74 Jul 6	297	79 Jun 5	346	82 Jul 9
199	70 Jan 29	249	74 Sep 10	298	79 Jul 5	347	82 Jul 12
200	70 Jan 31	250	74 Sep 12	299	79 Aug 3	348	82 Jul 19
201	70 Mar 6	251	74 Sep 19	300	79 Aug 17	349	82 Jul 22
202	70 Mar 7	252	74 Sep 23	301	79 Aug 21	350	82 Aug 14
203	70 Mar 23	253	74 Nov 5	302	79 Sep 8	351	82 Sep 4
204	70 Mar 25	254	75 Aug 3	303	79 Sep 14	352	82 Nov 22
205	70 Mar 29	255	75 Aug 21	304	79 Nov 15	353	82 Nov 26
206	70 May 30	256	75 Aug 22	305	79 Nov 21	354	82 Dec 7
207	70 Jun 25	257	76 Mar 23	306	80 Feb 6	355	82 Dec 14
208	70 Jul 7	258	76 Mar 28	307	80 Apr 4	356	82 Dec 17
209	70 Jul 23	259	76 Apr 30	308	80 Jul 5	357	82 Dec 19
210	70 Aug 11	260	76 Aug 22	309	80 Jul 17	358	82 Dec 25
211	70 Nov 5	261	77 Sep 7	310	80 Aug 6	359	82 Dec 26
212	70 Dec 11	262	77 Sep 9	311	80 Oct 15	360	83 Jan 6
213	70 Dec 24	263	77 Sep 16	312	80 Nov 14	361	83 Feb 3
214	71 Jan 24	264	77 Sep 19	313	80 Nov 23	362	83 Mar 10
215	71 Apr 1	265	77 Sep 24	314	81 Mar 7	363	83 Apr 15
216	71 Apr 6	266	77 Oct 12	315	81 Mar 25	364	83 Jun 14
217	71 Apr 20	267	77 Nov 22	316	81 Mar 30	365	84 Jan 31
218	71 Apr 22	268	77 Dec 27	317	81 Apr 1	366	84 Feb 16
219	71 May 16	269	78 Jan 1	318	81 Apr 3	367	84 Feb 17
220	71 Sep 1	270	78 Jan 8	319	81 Apr 10	368	84 Mar 7
221	71 Oct 3	271	78 Feb 13	320	81 Apr 14	369	84 Mar 10
222	71 Dec 14	272	78 Feb 25	321	81 Apr 24	370	84 Mar 14
223	72 Jan 10	273	78 Apr 8	322	81 Apr 28	371	84 Apr 24
224	72 Jan 20	274	78 Apr 11	323	81 Apr 30	372	84 May 22
225	72 Mar 5	275	78 Apr 16	324	81 May 4	373	84 May 31
226	72 Apr 17	276	78 Apr 19	325	81 May 8	374	85 Jan 21
227	72 Apr 18	277	78 Apr 21	326	81 May 10	375	85 Apr 24
228	72 May 28	278	78 Apr 28	327	81 May 16	376	85 Jul 2
229	72 Jun 8	279	78 Apr 29	328	81 Jul 20	377	85 Jul 9
230	72 Jun 16	280	78 Apr 30	329	81 Jul 24	378	85 Jul 17
231	72 Jul 19	281	78 May 7	330	81 Aug 7	379	86 Feb 4
232	72 Jul 22	282	78 May 11	331	81 Sep 17	380	86 Feb 6
233	72 Jul 23	283	78 May 31	332	81 Oct 7	381	86 Feb 7
234	72 Aug 2	284	78 Jun 22	333	81 Oct 12	382	86 Feb 10
235	72 Aug 4	285	78 Jul 10	334	81 Nov 14	383	86 Feb 14
236	72 Aug 7	286	78 Sep 7	335	81 Dec 5	384	86 Mar 6
237	72 Aug 11	287	78 Sep 23	336	81 Dec 9	385	86 May 4
238	72 Aug 16						

TABLE 3

NORMALIZED PEAK VALUES NEAR 154 DAYS

Data	Time interval	Peak Frequency	Normalized Peak value	Data source
Proton flares	78 Feb - 83 Aug	75 nHz	8.36	this work
Electron flares	78 Aug - 82 Dec	76 nHz	12.83	Droge et al. (1990)
HXRBS flares	80 Feb - 83 Dec	75 nHz	7.44	Dennis et al. (1985)
GRS flares	80 Feb - 83 Dec	75 nHz	8.87	Vestrand et al. (1987)

Table 4

OBSERVATIONS OF 154-DAY PERIODICITY[1]

Observed Activity	Cycle 19	20	21	References[2]
Gamma-ray Flares			Y	a
GOES Soft X-ray Flares			Y	a
HXRBS Flares			Y	b
Microwave Flares		Y[3]	Y	c
H-alpha Flares		Y[3]	Y	d
Flare Index		Y[3]	Y	e
Sunspot Area	Y[3]	Y	Y	f
Quiet Sun10-cm Radio Flux	N	Y	Y	f
Flares with I.P. Electrons			Y	g
Flares with I.P. Protons	Y	Y	Y	h
Flares selected by C.F.I.	51[d]	N		h, i, j
Flares selected by 10-cm Flux	51[d]	N	Y	j

Notes

1. The letter "Y" means yes, and "N" means no. Blank areas indicate either no measurements or no analyses. During cycle 20, the occurrence rates of flares selected by CFIs and by10-cm radio fluxes do not exhibit a154-day periodicity.
2. Reference code: a- Rieger et al. (1984); b-Kiplinger *et al.* (1984); c-Bogart and Bai (1985); d-Ichimoto *et al.* (1985); e-Özgüç and Ataç (1989); f-Lean and Brueckner (1989); g-Dröge *et al.* (1989); h-Present paper; i-Bai (1987); j-Kile, Cliver, and Fougere (1990).
3. The statistical significance is low for these cases.

REFERENCES

Akinyan, S.T., Bazilevskaya, G.A., Ishkov, V.N. et al. 1983, *Catalog of Solar Proton Events 1970-1979* (IZMIRAN: Moscow).

Bai T. 1987, *Ap. J. (Letters)* **318**, L85.

Bai, T., Cliver, E. W., and Kile, J. N. 1990, Proc. 21th Intern. Cosmic Ray Conf., **5**, p. 20, Adelaide, Australia.

Bai, T., and Sturrock, P. A. 1987, *Nature*, **327**, 601.

Bogart, R. S., and Bai, T. 1985, *Ap. J. (Letters)*, **299**, L51.

Brandt, S. 1976, *Statistical and Computational Methods in Data Analysis*, 2nd ed., (Amsterdam: North-Holland Pub. Co.)

Cooley, J. W., and Tukey, J. W. 1965, *Math. Comput.* **19**, 297.

Delache, P., Laclare, F., and Sadsaoud, H. 1985, Nature, 317, 416.

Dennis, B. R. 1985, Solar Phys. 100, 465.

Dennis, B. R., Orwig, L. E., Kiplinger, A. L., Gibson, B. R., Kennard, G. S., and Tolbert, A. K. 1985, *The Hard X-Ray Burst Spectrometer Event Listing,* NASA TM-86236.

Dodson, H. W., and Hedeman, E. R. 1971, *World Data Center for Solar-Terrestrial Physics Report* **UAG-14**, (Boulder: NOAA).

------. 1975, *World Data Center for Solar-Terrestrial Physics Report* **UAG-52**, (Boulder: NOAA).

------. 1981, *World Data Center for Solar-Terrestrial Physics Report* **UAG-80**, (Boulder: NOAA).

Droge, W. Gibbs, K., Grunsfeld, J. M., Meyer, P., and Newport, B. J. 1989, *Ap. J. Suppl.* (in pres)

Horne, J. H., and Baliunas, S. L. 1986, *Ap. J.* **302**, 757.

Ichimoto, K., Kubota, J., Suzuki, M., Tohmura, I., and Kurokawa, H. 1985, *Nature*, **316**, 422.

Kile, J. N., Cliver, E. W., and Fougere, P. F. 1990, *Ap. J.* (to be submitted)

Kiplinger, A. L., Dennis, B. R., and Orwig, L. E. 1984, *Bull. A. A. S.* **16**, 891.

Knight, J. W., Schatten, K. H., and Sturrock, P. A. 1979, *Ap. J. (Letters)* **227**. L153.

Lean, J. L., and Brueckner, G. E. 1989, Ap. J. **337**, 568.

Mardia, K. V. 1972, *Statistics of Directional Data*, (Acdemic Press: New York)

McKinnon, J.A. 1987, *Sunspot Numbers: 1610-1985*, Report UAG-95 (National Geophysical Data Center: Boulder, CO).

Ozguc A. & Atac T. 1989, *Solar Phys.* (in press).

Rieger, E., Share, G. H., Forrest, D. J., Kanbach, G., Reppin, C., and Chupp, E. L. 1984, *Nature*, **312**, 623.

Scargle, J. D. 1982, *Ap. J.* **263**, 835.

Shea, M.A., and D.F. Smart 1989, *Solar Phys.* (submitted).

Smart, D.F., and M.A. Shea 1971, *Solar Phys.* **16**, 484.

Solar Geophysical Data , 1980-87, Nos. **432-450** (Washington, DC: U.S. Department of Commerce).

Svestka Z. & Simon P. 1975, *Catalog of Solar Proton Events 1955-1969*, Reidel, Dordrecht

Thompson, J. M. T., and Stewart, H. B. 1986, *Nonlinear Dynamics and Chaos*, (John Wiley and Sons: New York)

Van Hollebeke, M.A.I., Ma Sung, L.S., and McDonald, F.B. 1975, *Solar Phys.* **41**, 189.

Vestrand, W. T., Forrest, D. J., Chupp, E. L., Rieger, E., and Share, G. H. 1987, *Ap. J.*, **322**, 1010.

Wolff, C. L. 1983, *Ap. J.* **264**, 667.

FIGURE CAPTIONS

Fig. 1--Normalized power spectra of the proton flare occurrence rate.

Fig. 2--Rayleigh power distribution. The vertical axis is the number of frequencies for which the Rayleigh power exceeds X. The straight line is the fit to the points for lower values of Rayleigh power.

Fig. 3--The logarithimic likelihood function as a function of the last event number (see eq. 10 for the definition). Notice that the logarithmic likelihood function increases almost linearly between events 270 and 370. The momentary decrease of the likelihood in the interval for event numbers between 325 and 340 is due to the two misbehaving 154-day cycles around t=9830 days (see Fig. 4).

Fig. 4--Smoothed occurrence rate of proton flares for the interval between 1977 September 14 and 1984 November 9. The periodic modulation is semi-regular for 13 cycles from 1978 February 8 through 1983 August 6, except for two cycles around day 9830.

Fig. 5--Normalized power spectra of the proton flare occuurrence rate.

Fig. 6--Smoothed occurrence rate of proton flares for the interval from 1958 Jan 1 to 1972 May 22. The positions of vertical grid lines, which are 154.6 days apart, are chosen such that the peak phase falls near the mid points. Notice that the 154.6-day periodicity is semi-regular for 33 consecutive cycles, with only a few irregular cycles.

Fig. 7--Yearly number of proton flares. The two epochs when the 154-day periodicity was operative are shown by two horizontal lines in the upper part of the figure. The occurrence rate shows a dip near the maximum of cycle 19 and also near the maximum of cycle 21.

Fig. 8--Phase diagrams for the two epochs when the 154-day periodicity was in operation. Notice large amplitudes of modulation and a phase shift of about 0.5. The beginning of 1955 is chosen as the zero phase.

Fig. 9--Time shift between the 154-day periodicity of the two epochs. The solid dot indicates the location (T=154.6 days, Δt=77 days) where the power is the strongest. The contour line indicates the parameter range of one standard deviation

Fig. 10--Smoothed occurrence rate of proton flares for the interval from the beginning of 1972 to the end of 1977. Vertical grid lines are 154.6 days apart. During this interval, the proton flare rate shows no periodic modulation.

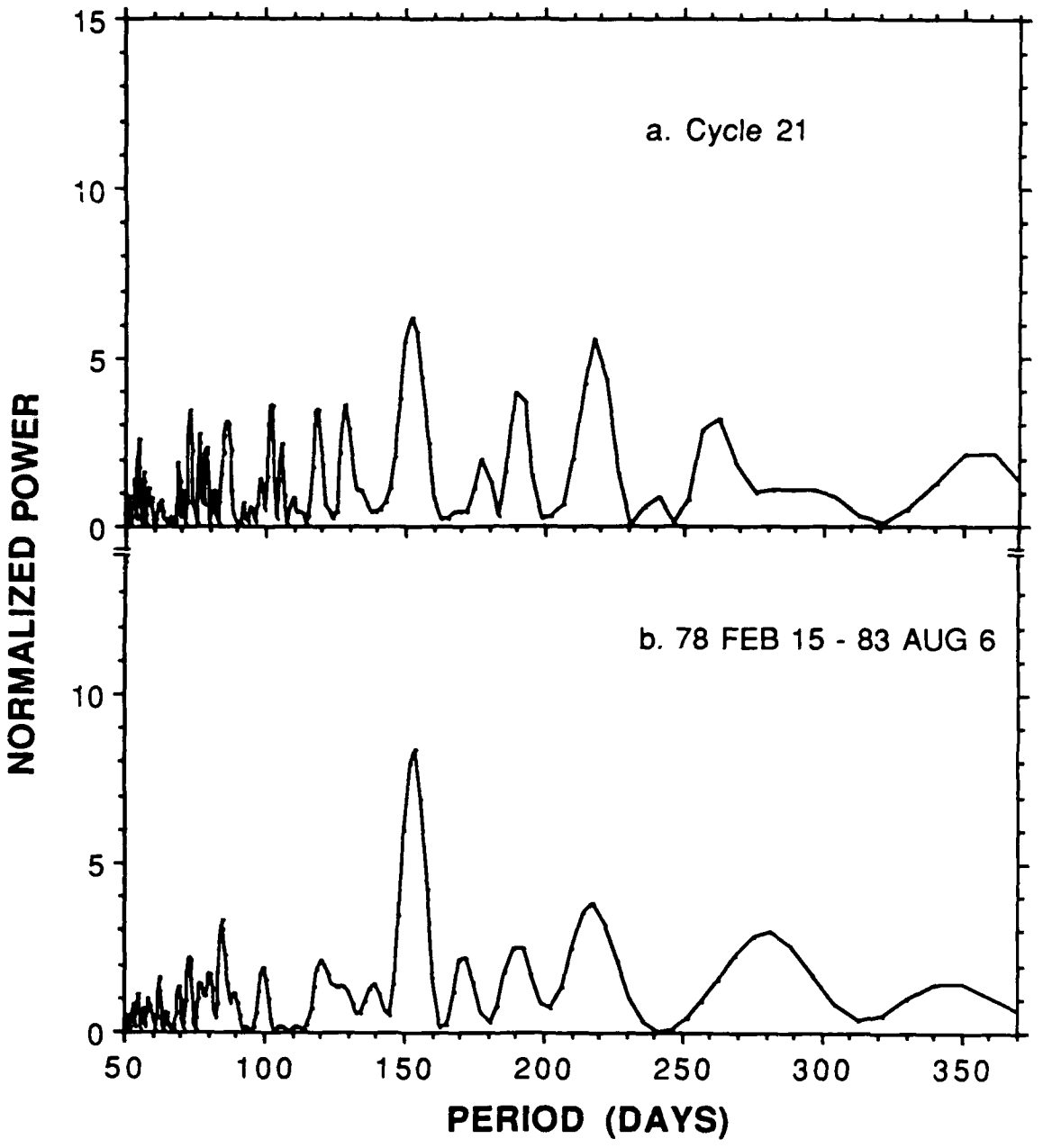
15
10
5
0
a. Cycle 21
b. 78 FEB 15 - 83 AUG 6
10
5
0
NORMALIZED POWER
50
100
150
200
250
300
350
PERIOD (DAYS)

Fig. 1

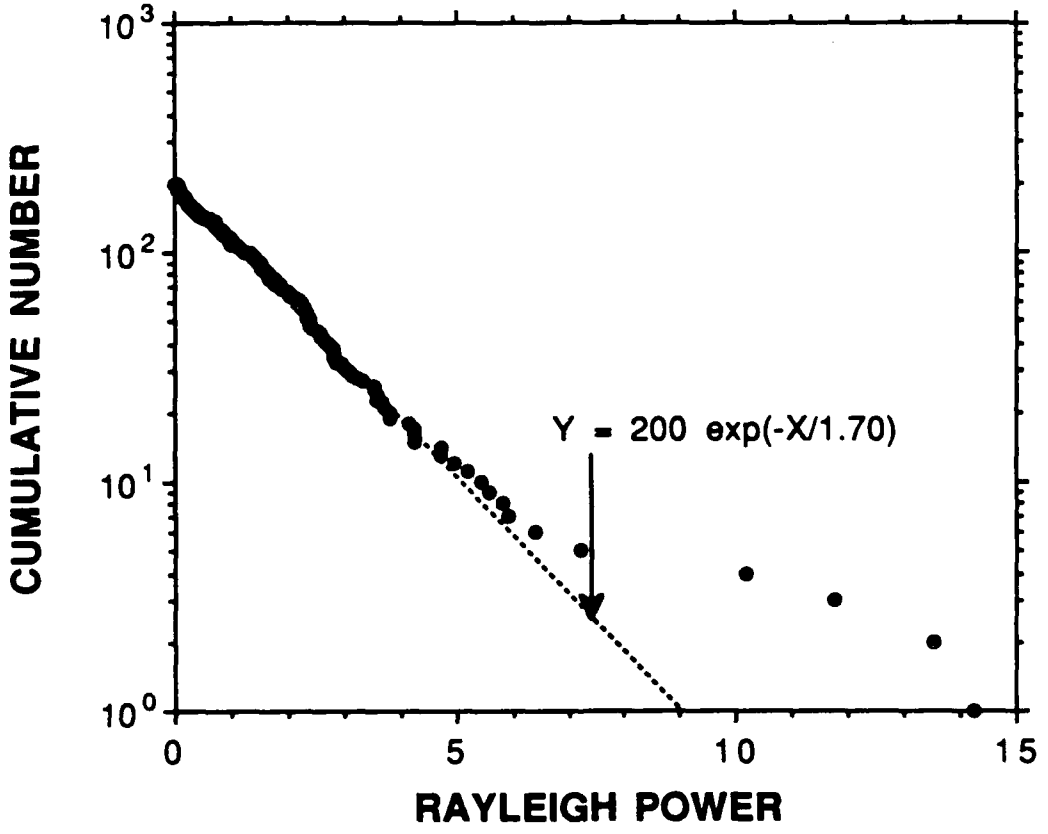
CUMULATIVE NUMBER
10^3
10^2
10^1
10^0
Y = 200 exp(-X/1.70)
0
5
10
15
RAYLEIGH POWER

Fig. 2

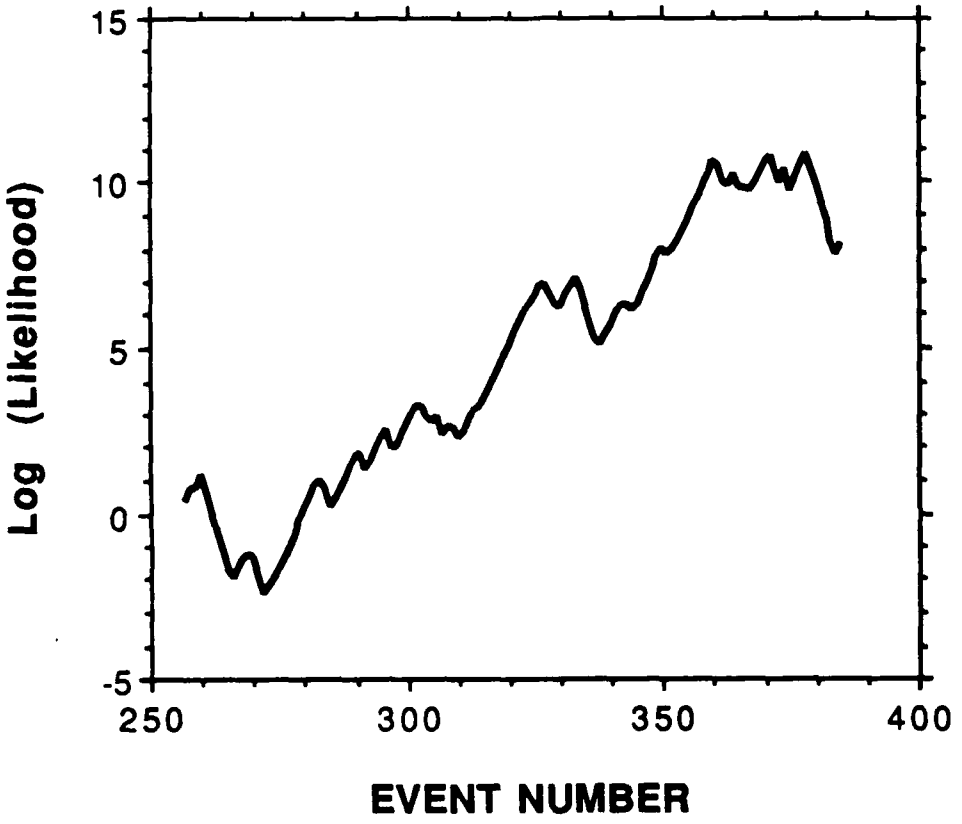

Fig. 3

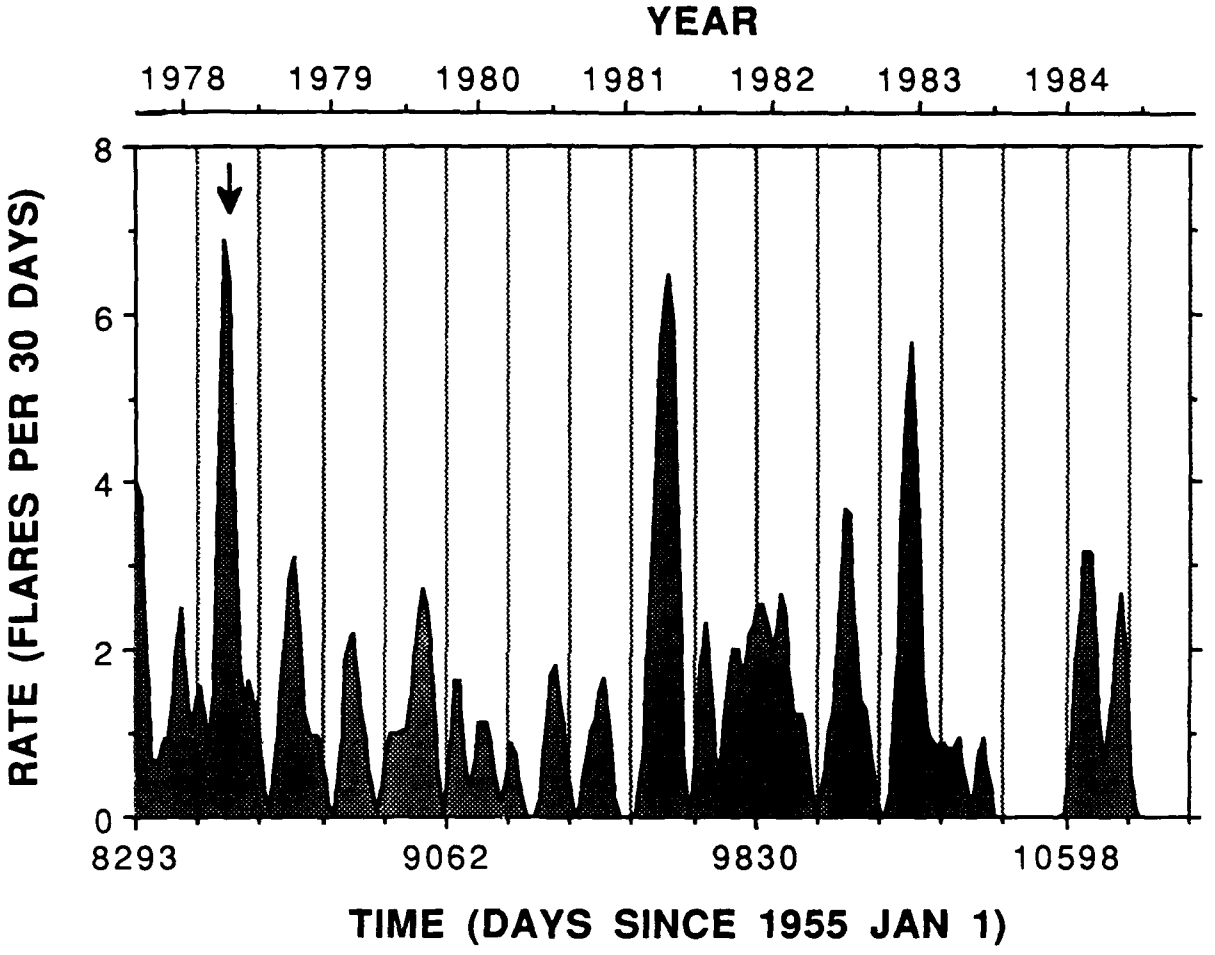
YEAR
1978
1979
1980
1981
1982
1983
1984
RATE (FLARES PER 30 DAYS)
0
2
4
6
8
8293
9062
9830
10598
TIME (DAYS SINCE 1955 JAN 1)

Fig. 4

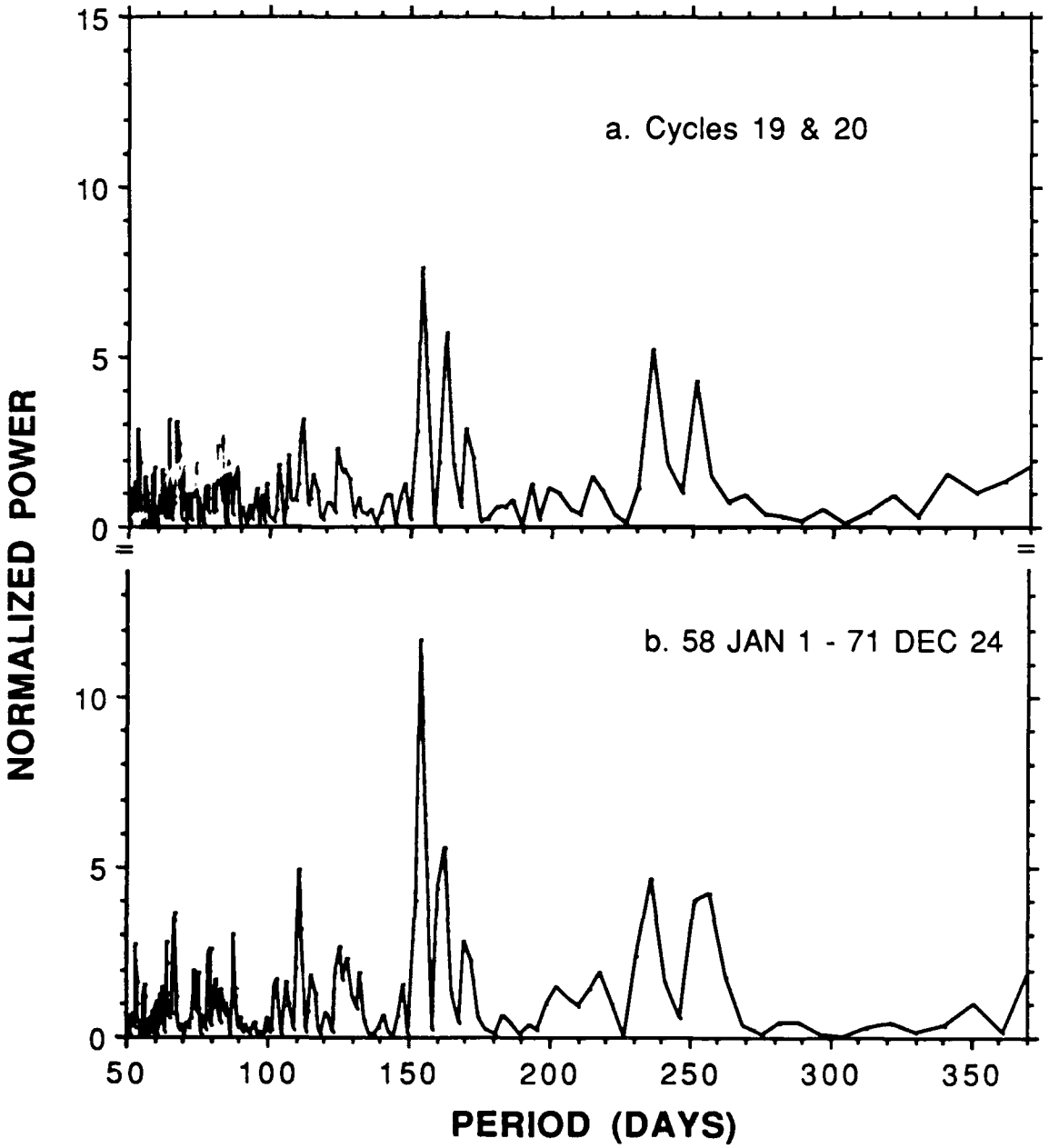
15
10
5
0
a. Cycles 19 & 20
b. 58 JAN 1 - 71 DEC 24
NORMALIZED POWER
10
5
0
50
100
150
200
250
300
350
PERIOD (DAYS)

Fig. 5

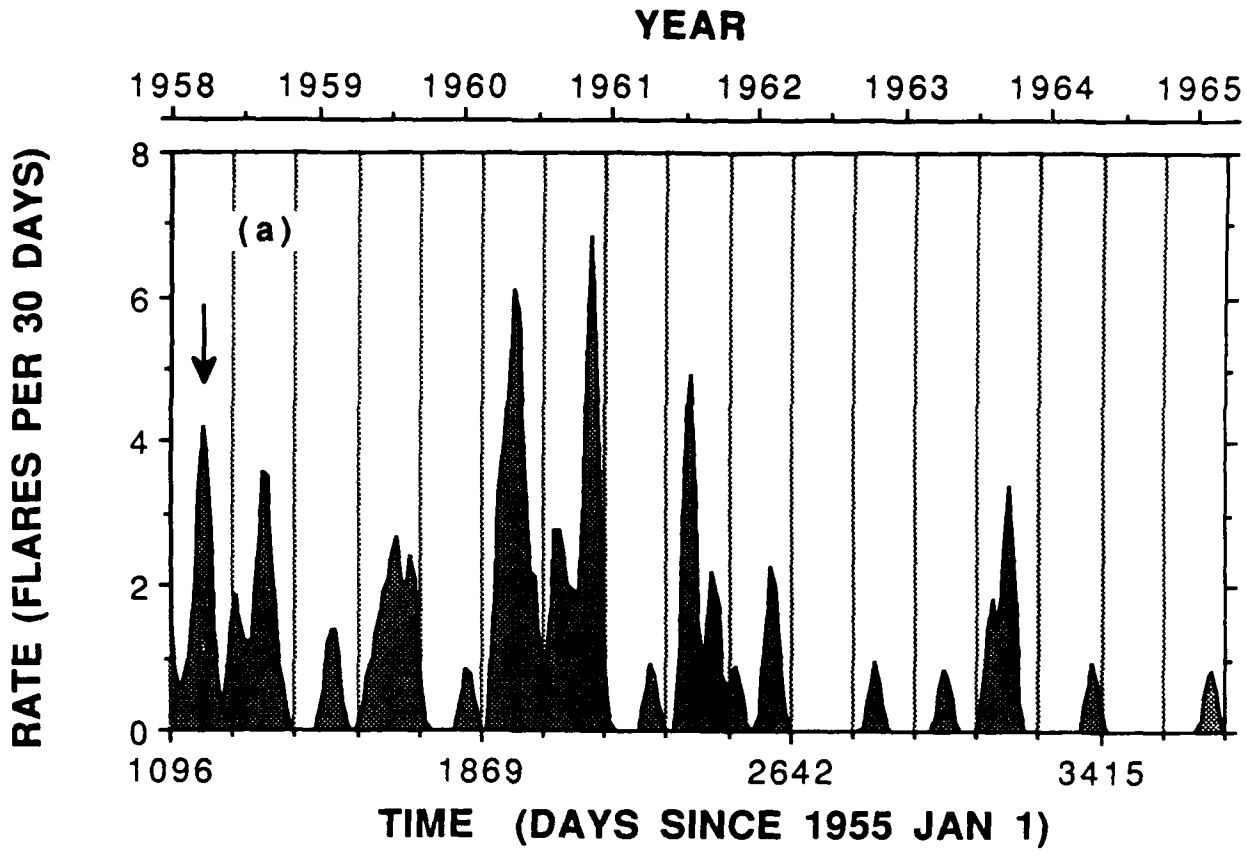
YEAR
1958
1959
1960
1961
1962
1963
1964
1965
(a)
RATE (FLARES PER 30 DAYS)
8
6
4
2
0
1096
1869
2642
3415
TIME (DAYS SINCE 1955 JAN 1)

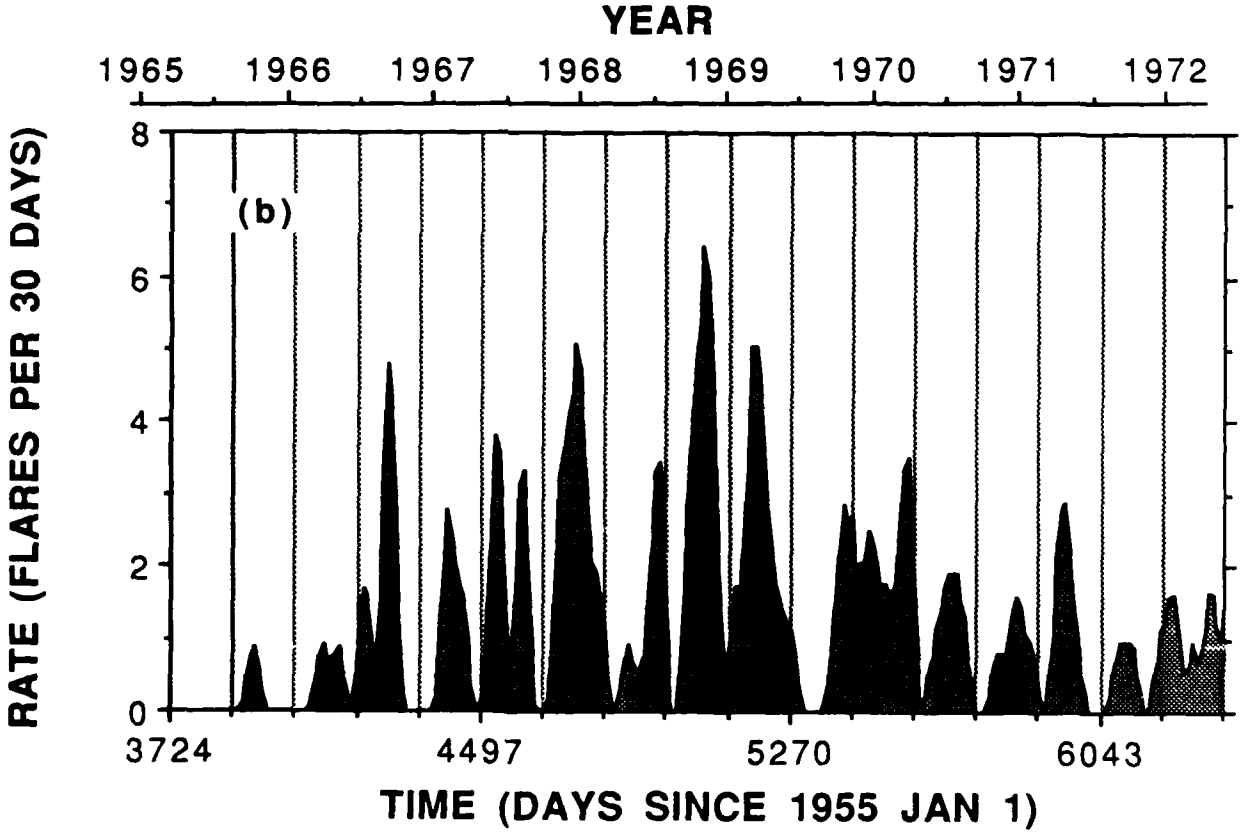
YEAR
1965
1966
1967
1968
1969
1970
1971
1972
(b)
RATE (FLARES PER 30 DAYS)
8
6
4
2
0
3724
4497
5270
6043
TIME (DAYS SINCE 1955 JAN 1)

Fig. 6

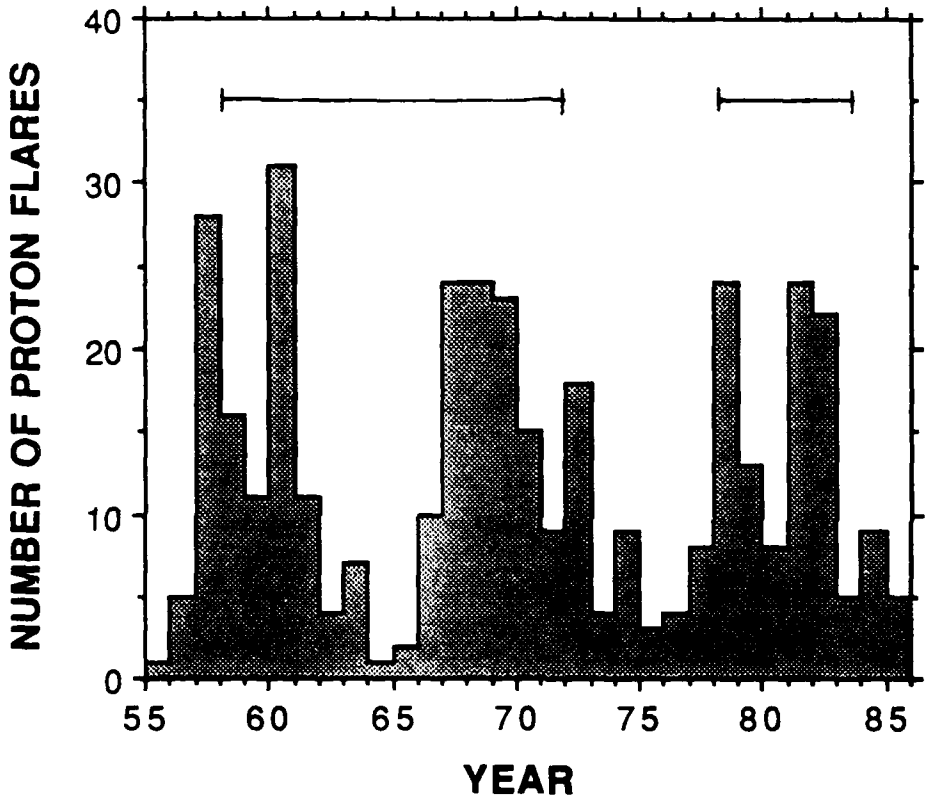

Fig. 7

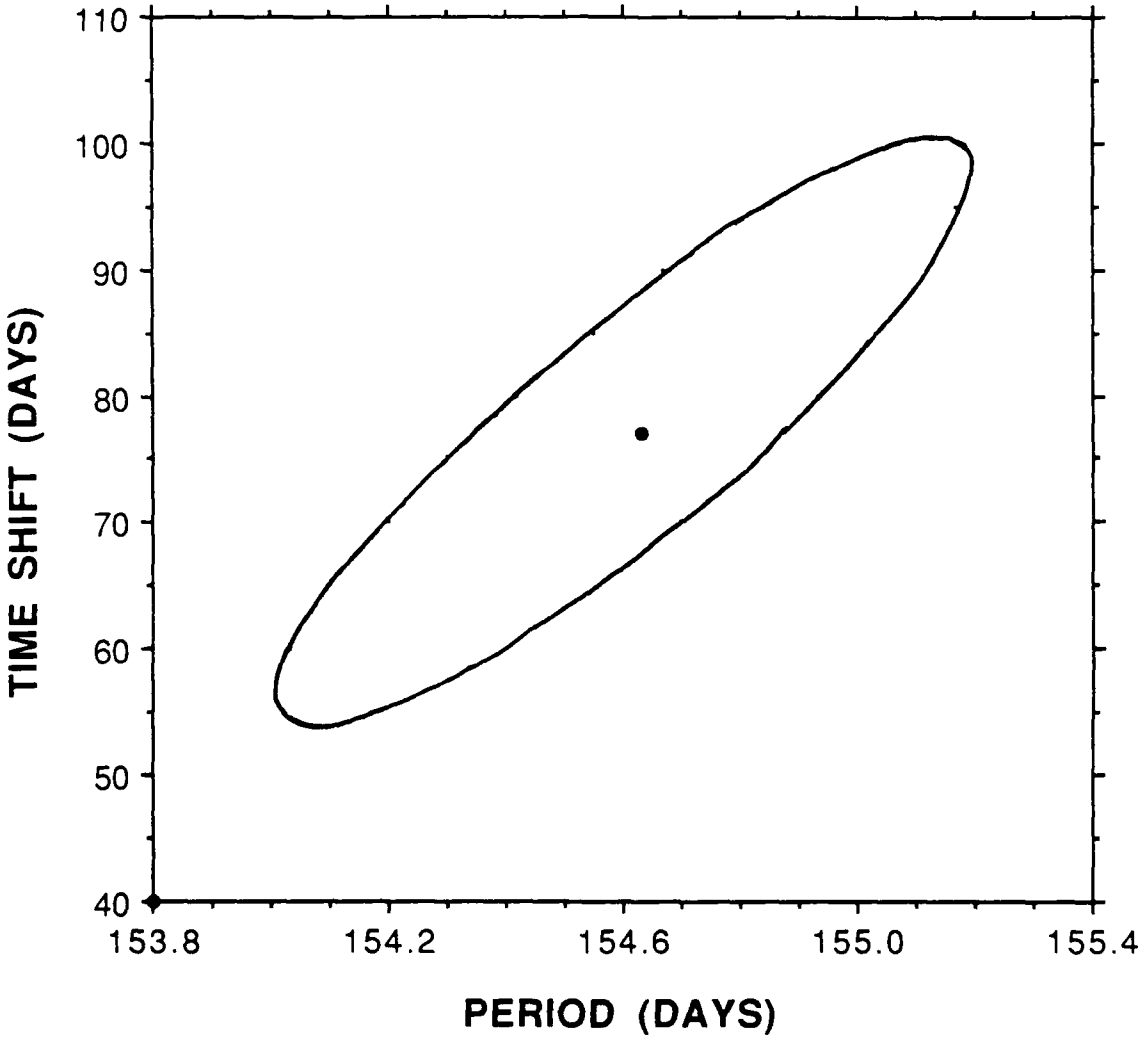
110
100
90
80
70
60
50
40
TIME SHIFT (DAYS)
153.8
154.2
154.6
155.0
155.4
PERIOD (DAYS)

Fig. 8

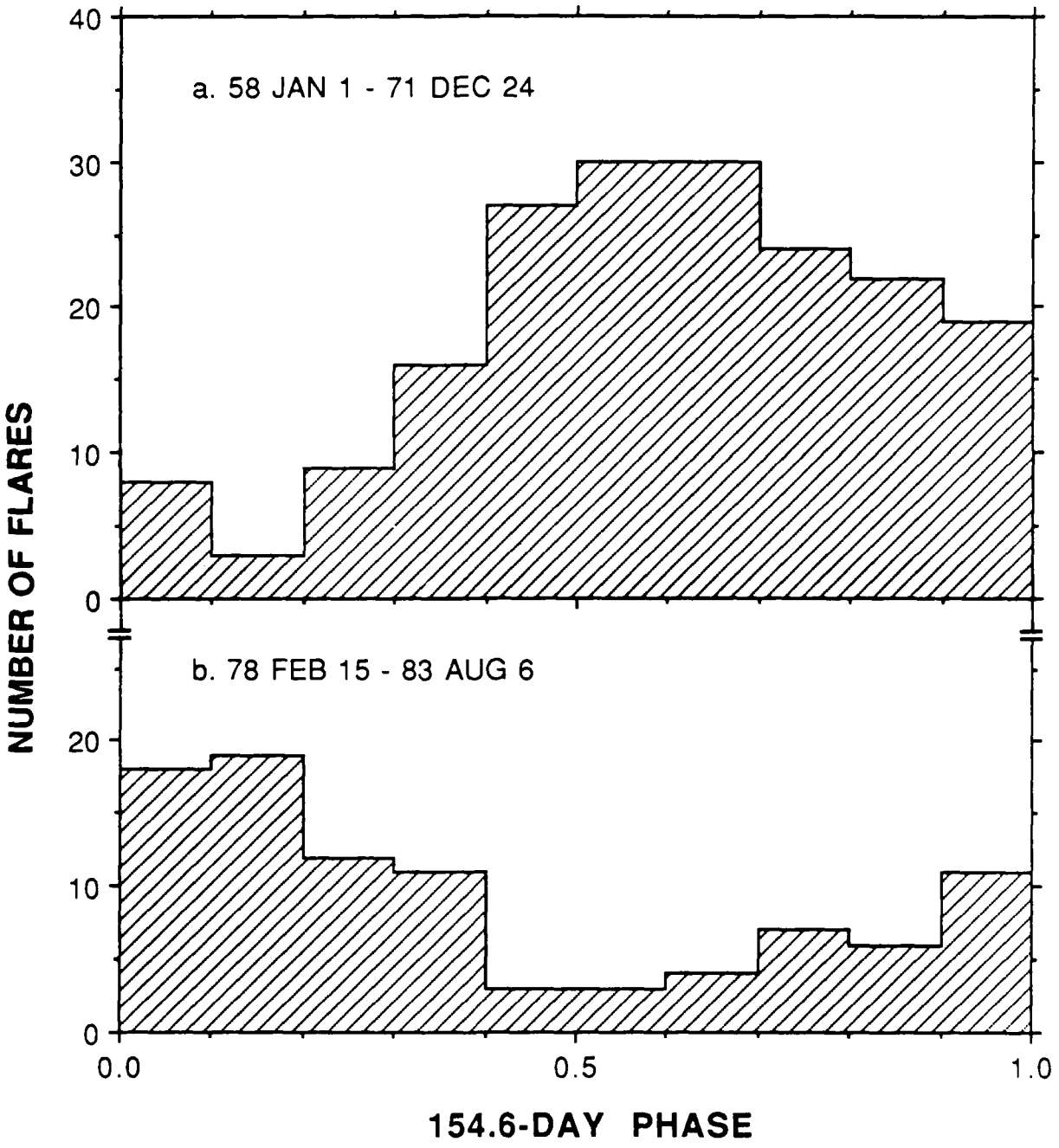
40
30
20
10
0
a. 58 JAN 1 - 71 DEC 24
20
10
0
b. 78 FEB 15 - 83 AUG 6
NUMBER OF FLARES
0.0
0.5
1.0
154.6-DAY PHASE

Fig. 9

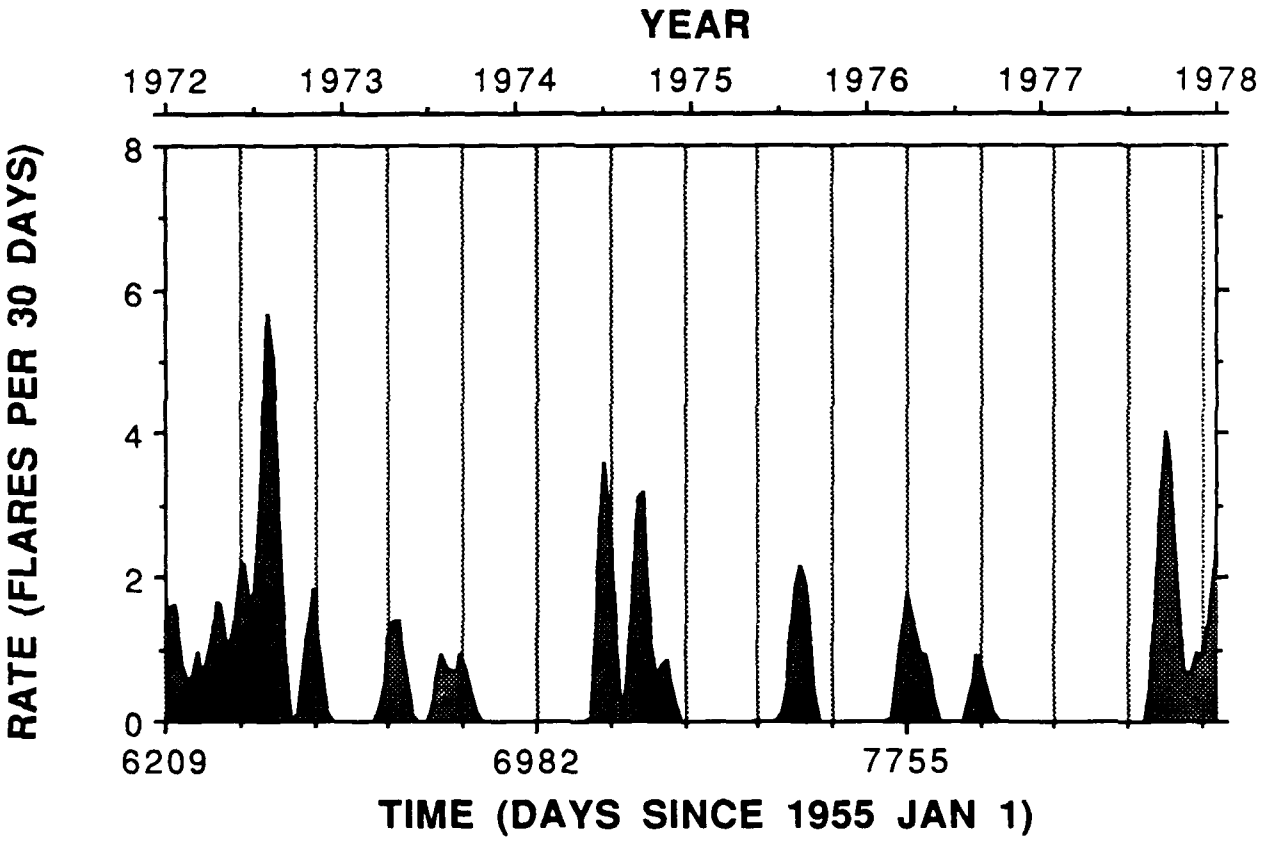
YEAR
1972
1973
1974
1975
1976
1977
1978
RATE (FLARES PER 30 DAYS)
8
6
4
2
0
6209
6982
7755
TIME (DAYS SINCE 1955 JAN 1)

Fig. 10